Pergamon

Ann. Nucl. Energy, Vol. 25, No. 8, pp. 507–528, 1998

PII: S0306-4549(97)00078-9
Printed in Great Britain
0306-4549/98 $19.00 + 0.00

NODAL NEUTRON KINETICS MODEL BASED ON NONLINEAR ITERATION PROCEDURE FOR LWR ANALYSIS

VYACHESLAV G. ZIMIN* and HISASHI NINOKATA

Research Laboratory for Nuclear Reactors, Tokyo Institute of Technology, O-okayama, Meguro-ku, Tokyo 152, Japan

(Received 30 June 1997)

Abstract—A 3-dimensional neuron kinetics model based on the analytical nodal method and nonlinear iteration procedure is developed for Light Water Reactor (LWR) transient calculations. The solution procedure is decoupled on a local solution of the nodal equations for two-node problems and global iterations of the coarse-mesh finite-difference method. An orthogonality of the basic functions used for the neutron flux expansion results in an efficient algorithm of the solution of the nodal equations for the two-node problem. The initial system of $8G$ nodal equations is reduced to a set of G and $2G$ equations, where G is a number of neutron energy groups. A fully implicit scheme with an analytical treatment of the delayed neutron precursors equations is used for time integration. An adaptive time-step size control procedure based on the time-step doubling technique is applied. The described numerical methods are implemented into the computer code SKETCH-N. The 3D LWR Langenbuch–Maures–Werner (LMW) operational transient and 2D and 3D Boiling Water Reactor (BWR) LRA super-prompt-critical benchmark problems are calculated in order to verify the code. A comparison of the computed results with the solutions obtained by the other nodal computer codes demonstrate fidelity and efficiency of the SKETCH-N code. © 1998 Elsevier Science Ltd.

1. INTRODUCTION

LWR licensing safety analysis, operational support and operator training require accurate and fast computer codes for the dynamics calculations. There is general agreement that a 3-dimensional neutron kinetics model is necessary to obtain satisfactory results for many LWR transients. An excellent review paper about numerical methods used in the modern

*Author for correspondence. Current address: Thermal Hydraulics Safety Research Laboratory, Department of Reactor Safety Research, Japan Atomic Energy Research Institute, Tokai-mura, Naka-gun, Ibaraki-ken, 319-11, Japan. Fax: +81-29-282-6728, E-mail: slava@ls+f3.tokai.jaeki.go.jp

neutron kinetics codes was published recently (Sutton and Aviles, 1996). The current introduction outlines only the numerical methods somehow related to our work.

The paper presents nodal neutron kinetics computer code SKETCH-N developed for the LWR transient calculations. The numerical methods used in the code are described and the results of the LWR neutron kinetics benchmark problem calculations are given. The mathematical model of the code is based on the analytical nodal method with the nonlinear iteration procedure. The nonlinear iteration procedure is proposed by K. S. Smith (1984) in order to improve the efficiency of the traditional nodal methods (Lawrence, 1986). In this approach nodal equations are used only locally for the solution of the two-node problems which contain two adjacent nodes with common interface. The global solution procedure is based on the coarse-mesh finite-difference (CMFD) formulation of the neutron diffusion equations. The CMFD coupling coefficients are determined from the condition that the CMFD method reproduces the same surface-averaged neutron current as the nodal method. As a result the solution procedure is decoupled on a local solution of the nodal equations for two-node problems and global iterations of the CMFD method. The first advantage of the nonlinear iteration procedure is a reduction in the computer memory requirements in comparison with the traditional nodal methods, because the nodal equations are solved locally and there is no need to save the neutron flux expansion coefficients (Smith, 1984). The computing time can be also decreased because the efficient iterative methods developed for the finite-difference codes can be also applied for the solution of the global CMFD equations (Al-Chalabi and Turinsky, 1994; Yang *et al.*, 1993; Zimin and Ninokata, 1996). Another reason of the effectiveness of the nonlinear iteration procedure is that during neutron kinetics calculations there is only a few expensive recalculations of CMFD coefficients at each time-step (Joo and Downar, 1996). The efficient numerical algorithms are also developed for the solution of the nodal equations for two-node problems (Engrand *et al.*, 1992, Zimin and Ninokata, 1997). With G being a number of neutron energy groups, the original $8G$ nodal equations are reduced to a set of $2G$ and $4G$ equations in the case of the nodal expansion method (NEM) (Engrand, *et al.*, 1992) and to G and $2G$ equations with the nodal method based on Legendre polynomials (Zimin and Ninokata, 1997, Zimin, 1997). The nonlinear iteration procedure is widely used in the many neutron kinetics code with the different nodal methods: in the NESTLE (Al-Chalabi *et al.*, 1993), SPANDEX (Aviles, 1993) and PARCS (Joo *et al.*, 1996) codes with NEM and in the SIMULATE-3K (Borkowski *et al.*, 1996) code with the semi-analytical nodal method. The mathematical model of the SKETCH-N code is also used the nonlinear iteration procedure with the recently developed analytical nodal method (Zimin, 1997).

The time integration method employed in the SKETCH-N code is a fully implicit scheme applied to the neutron flux equations in combination with an analytical treatment of the delayed neutron precursor equations (Stacey, 1969). An adaptive time-step selection providing an accurate and efficient solution is an important problem for the widely varying LWR transients (Aviles, 1994). An automatic time-step size control procedure based on the time-step doubling technique (Crouzet and Turinsky, 1996) is incorporated into the code. A time-step size selection is based on the requirement to held a temporal truncation error below a given tolerance. The temporal truncation error is estimated by the Richardson extrapolation of two solutions calculated with different time-step sizes.

Any implicit method of time discretization results in a large system of equations which have to be solved at each time-step. The solution of the CMFD equations in the

SKETCH-N code is organized using a traditional way of the outer and inner iterations. The Chebyshev acceleration procedure (Zimin and Ninokata, 1996) is used as an outer iteration technique. The procedure allows to realize two iterative methods: the traditional Chebyshev semi-iterative method (Hageman and Young, 1981) and the Chebyshev semi-analytical (CSA) method (Zimin and Ninokata, 1996). In the CSA method the Chebyshev polynomials are used for the acceleration of the secondary iterative process, where the residual vectors converge to the first eigenvector of the iteration matrix. When the convergence of the secondary iterative process is attained, the iterative approximation is refined by adding an error vector to the obtained solution. The SSOR method (Hageman and Young, 1981) is applied as an inner iteration technique.

This paper is organized as follows. An application of the analytical nodal method for the steady-state fixed source problem (FSP) and an implementation of the nodal coupling into the CMFD method are presented in Section 2. Section 3 describes the fully implicit scheme used in the SKETCH-N code and shows how to transform the resulting time-discretized equations into the FSP formulation. The Section 4 presents an automatic step size control procedure based on the time-step doubling technique. The three-level iterative procedure used for the solution of the neutron kinetics equations at each time-step is described in Section 5. The numerical results of the LWR delayed-critical and super-prompt critical transient calculations and their comparison with the results of the other nodal neutron kinetics codes are given in Section 6. A summary and conclusions are presented in Section 7.

2. NONLINEAR ANALYTICAL NODAL METHOD FOR THE STEADY-STATE FIXED SOURCE PROBLEM

The polynomial and analytical nodal methods have been recently developed and applied for the steady-state neutron diffusion calculations (Zimin and Ninokata, 1997, Zimin, 1997). The polynomial method is based on the neutron flux expansion into Legendre polynomials. The Legendre polynomials up to the second order and the modified hyperbolic sinus and cosines are used as basic functions in the analytical nodal method. An application of the nodal methods to the steady-state FSP is straightforward and here we present the equations of the analytical nodal method. The FSP is interesting by itself for the calculations of subcritical systems with an external source (Ishii and Sano, 1996) and for the numerical solution of the neutron kinetics equations as it will be shown in the following Section 3. The steady-state transverse-integrated neutron diffusion equations of the FSP can be written as follows:

$$-D_g^k \frac{d^2}{dx^2}\Phi_g^k(x) + \Sigma_{Rg}^k \Phi_g^k(x) = \chi_g \sum_{g'=1}^{G} \nu\Sigma_{fg'}^k \Phi_{g'}^k(x) + \sum_{g' \neq g}^{G} \Sigma_{sg' \to g}^k \Phi_{g'}^k(x) - \frac{1}{\Delta y_k} L_{gy}^k(x) - \frac{1}{\Delta z_k} L_{gz}^k(x) + S_g^k(x)$$

where the x-direction is considered as an example; g is index of the energy neutron group; k is the index of the node $[-\Delta x_k/2, \Delta x_k/2]x[-\Delta y_k/2, \Delta y_k/2]x[-\Delta z_k/2, \Delta z_k/2]$; $\Phi_g^k(x)$ is the transverse integrated neutron flux; $L_{gy}^k(x)$, $L_{gz}^k(x)$ are the transverse leakages in y and z directions, respectively; $S_g^k(x)$ is the transverse integrated source term; all other notations are fairly standard.

The analytical basic functions employed are Legendre polynomials up to the second order and the modified hyperbolic sinus and cosine proposed by Hennart (1988) for the higher order nodal schemes :

$$P_0(t) = 1$$

$$P_1(t) = t$$

$$P_2(t) = \frac{1}{2}(3t^2 - 1)$$

$$P_3(t) = \frac{1}{\sinh(\alpha_{gx}^k) - m_{gx1}^k(\sinh)}\left[\sinh(\alpha_{gx}^k t) - m_{gx1}^k(\sinh)P_1(t)\right]$$

$$P_4(t) = \frac{1}{\cosh(\alpha_{gx}^k) - m_{gx0}^k(\cosh) - m_{gx2}^k(\cosh)}\left[\cosh(\alpha_{gx}^k t) - m_{gx0}^k(\cosh)P_0(t) - m_{gx2}^k(\cosh)P_2(t)\right]$$

where

$$t = 2x/\Delta x_k \qquad \alpha_{gx}^k = \sqrt{\frac{\Sigma_{Rg}^k}{D_g^k}}\frac{\Delta x_k}{2} \qquad m_{gx1}^k(\sinh) = \frac{1}{N_1}\int_{-1}^{1} \sinh(\alpha_{gx}^k t)\, P_1(t)\mathrm{d}t$$

$$m_{gxi}^k(\cosh) = \frac{1}{N_i}\int_{-1}^{1} \cosh(\alpha_{gx}^k t)\, P_i(t)\mathrm{d}t, \text{ for } i = 0, 2 \qquad N_i = 2/(2i+1), \text{ for } i = 0, 1, 2.$$

The basic functions are mutually orthogonal at the interval $[-1, 1]$ and normalized to unity at $t = 1$. As it will be shown below an orthogonality of the basic functions results in an efficient algorithm of the nodal equations solution.

The transverse-integrated neutron flux is expanded over the node into the basic functions as

$$\Phi_g^k(x) = \overline{\Phi}_g^k + \sum_{i=1}^{4} a_{gxi}^k P_i(2x/\Delta x_k)$$

where $\overline{\Phi}_g^k$ is the average over the node neutron flux.

The transverse leakages and the external source term are also expanded up to the second order using the quadratic leakage approximation (Bennewitz *et al.*, 1975) as:

$$L_{gy}^k(x) = \overline{L}_{gy}^k + \sum_{i=1}^{2} \rho_{gyxi}^k P_i(2x/\Delta x_k); \qquad L_{gz}^k(x) = \overline{L}_{gz}^k + \sum_{i=1}^{2} \rho_{gzxi}^k P_i(2x/\Delta x_k);$$

$$S_g^k(x) = \overline{S}_g^k + \sum_{i=1}^{2} s_{gxi}^k P_i(2x/\Delta x_k).$$

The average over the node neutron flux, the transverse leakage expansion coefficients and the source term expansion coefficients are assumed to be known from the results of CMFD iterations. The other neutron flux expansion coefficients can be obtained from the

solution of the two-node problems. The two-node problem is obtained considering two nodes which have the common interface. In order to calculate $8G$ unknowns of the 2-node problem (2 node $\times$ 4 neutron flux expansion coefficients $\times$ G neutron energy groups) the following equations are used: *2G neutron balance equations, 2G first-order moment-weighting equations, 2G second-order moment-weighting equations and 2G equations of the neutron flux and neutron current continuity* at the internal interface between two nodes. After some algebra the resulting analytical nodal equations are given in the following:
First-order moment-weighting equations (weighting with $P_1(t)$):

$$a^k_{gx3} = \frac{\sinh(\alpha^k_{gx}) - m^k_{gx1}(\sinh)}{\Sigma^k_{Rg} m^k_{gx1}(\sinh)} \left[\Sigma^k_{Rg} a^k_{gx1} - \chi_g \sum_{g'=1}^{G} \nu\Sigma^k_{fg'} a^k_{g'x1} - \sum_{g' \neq g}^{G} \Sigma^k_{sg' \to g} a^k_{g'x1} + \frac{1}{\Delta y_k} \rho^k_{gyx1} + \frac{1}{\Delta z_k} \rho^k_{gzx1} + s^k_{gx1} \right] \tag{1}$$

Second-order moment-weighting equations (weighting with $P_2(t)$):

$$a^k_{gx4} = \frac{\cosh(\alpha^k_{gx}) - m^k_{gx0}(\cosh) - m^k_{gx2}(\cosh)}{\Sigma^k_{Rg} m^k_{gx2}(\cosh)} \left[\Sigma^k_{Rg} a^k_{gx2} - \chi_g \sum_{g'=1}^{G} \nu\Sigma^k_{fg'} a^k_{g'x2} - \sum_{g' \neq g}^{G} \Sigma^k_{sg' \to g} a^k_{g'x2} + \frac{1}{\Delta y_k} \rho^k_{gyx2} + \frac{1}{\Delta z_k} \rho^k_{gzx2} + s^k_{gx2} \right] \tag{2}$$

Substituting the expression for the fourth moment into *the neutron balance equation* we obtain a system of G equations with respect to the second moment of each node:

$$\Sigma^k_{Rg} a^k_{gx2} \left[\frac{m^k_{gx0}(\cosh)}{m^k_{gx2}(\cosh)} \right] - \left[\frac{\chi_g}{k_{\text{eff}}} \sum_{g'=1}^{G} \nu\Sigma^k_{fg'} a^k_{g'x2} + \sum_{g' \neq g}^{G} \Sigma^k_{sg' \to g} a^k_{g'x2} \right] \left[\frac{m^k_{gx0}(\cosh)}{m^k_{gx2}(\cosh)} - \frac{3}{\left(\alpha^k_{gx}\right)^2} \right]$$

$$= \Sigma^k_{Rg} \bar{\Phi}^k_g - \chi_g \sum_{g'=1}^{G} \nu\Sigma^k_{fg'} \bar{\Phi}^k_{g'} - \sum_{g' \neq g}^{G} \Sigma^k_{sg' \to g} \bar{\Phi}^k_{g'} + \frac{1}{\Delta y_1} \bar{L}^k_{gy} + \frac{1}{\Delta z_1} \bar{L}^k_{gz} - \bar{S}^k_g$$

$$- \left(\frac{1}{\Delta y_k} \rho^k_{gyx2} + \frac{1}{\Delta z_k} \rho^k_{gzx2} - s^k_{gx2} \right) \left[\frac{m^k_{gx0}(\cosh)}{m^k_{gx2}(\cosh)} - \frac{3}{\left(\alpha^k_{gx}\right)^2} \right].$$

Substituting the expression for third moment into the *neutron flux and neutron current continuity equations* we obtain system of $2G$ equations with respect to the first moments of the two-node problem as shown in the following:

Flux continuity equation:

$$a^k_{gx1}\left(\frac{\sinh\left(\alpha^k_{gx}\right)}{m^k_{gx1}(\sinh)}\right)-\frac{1}{\Sigma^k_{Rg}}\left(\frac{\sinh\left(\alpha^k_{gx}\right)}{m^k_{gx1}(\sinh)}-1\right)\left[\chi_g\sum_{g'=1}^{G}\nu\Sigma^k_{fg'}a^k_{g'x1}+\sum_{g'\neq g}^{G}\Sigma^k_{sg'\to g}a^k_{g'x1}\right]$$

$$+a^{k+1}_{gx1}\left(\frac{\sinh\left(\alpha^{k+1}_{gx}\right)}{m^{k+1}_{gx1}(\sinh)}\right)-\frac{1}{\Sigma^{k+1}_{Rg}}\left(\frac{\sinh\left(\alpha^{k+1}_{gx}\right)}{m^{k+1}_{gx1}(\sinh)}-1\right)\left[\chi_g\sum_{g'=1}^{G}\nu\Sigma^{k+1}_{fg'}a^{k+1}_{g'x1}+\sum_{g'\neq g}^{G}\Sigma^{k+1}_{sg'\to g}a^{k+1}_{g'x1}\right]$$

$$=\overline{\Phi}^{k+1}_g+a^{k+1}_{gx2}+a^{k+1}_{gx4}-\frac{1}{\Sigma^{k+1}_{Rg}}\left(\frac{\sinh\left(\alpha^{k+1}_{gx}\right)}{m^{k+1}_{gx1}(\sinh)}-1\right)\left[\frac{1}{\Delta y_{k+1}}\rho^{k+1}_{gyx1}+\frac{1}{\Delta z_{k+1}}\rho^{k+1}_{gzx1}-s^{k+1}_{gx1}\right]$$

$$-\overline{\Phi}^k_g-a^k_{gx2}-a^k_{gx4}-\frac{1}{\Sigma^k_{Rg}}\left(\frac{\sinh\left(\alpha^k_{gx}\right)}{m^k_{gx1}(\sinh)}-1\right)\left[\frac{1}{\Delta y_k}\rho^k_{gyx1}+\frac{1}{\Delta z_k}\rho^k_{gzx1}-s^k_{gx1}\right]$$

Current continuity equation:

$$-\frac{2D^k_g}{\Delta x_k}\left\{\left(\frac{\alpha^k_{gx}\cosh\left(\alpha^k_{gx}\right)}{m^k_{gx1}(\sinh)}\right)a^k_{gx1}-\frac{1}{\Sigma^k_{Rg}}\left(\frac{\alpha^k_{gx}\cosh\left(\alpha^k_{gx}\right)}{m^k_{gx1}(\sinh)}-1\right)\left(\chi_g\sum_{g'=1}^{G}\nu\Sigma^k_{fg'}a^k_{g'x1}+\sum_{g'\neq g}^{G}\Sigma^k_{sg'\to g}a^k_{g'x1}\right)\right\}$$

$$+\frac{2D^{k+1}_g}{\Delta x_{k+1}}\left\{\left(\frac{\alpha^{k+1}_{gx}\cosh\left(\alpha^{k+1}_{gx}\right)}{m^{k+1}_{gx1}(\sinh)}\right)a^{k+1}_{gx1}-\frac{1}{\Sigma^{k+1}_{Rg}}\left(\frac{\alpha^{k+1}_{gx}\cosh\left(\alpha^{k+1}_{gx}\right)}{m^{k+1}_{gx1}(\sinh)}-1\right)\left(\chi_g\sum_{g'=1}^{G}\nu\Sigma^{k+1}_{fg'}a^{k+1}_{g'x1}+\sum_{g'\neq g}^{g}\Sigma^{k+1}_{g'x1}a^{k+1}_{g'x1}\right)\right\}$$

$$=\frac{2D^k_g}{\Delta x_k}\left[3a^k_{gx2}+\frac{\left(\alpha^k_{gx}\sinh(\left(\alpha^k_{gx}\right)-3m^k_{gx2}(\cosh)\right)}{\left(\cosh\left(\alpha^k_{gx}\right)-m^k_{gxo}(\cosh)-m^k_{gx2}(\cosh)\right)}a^k_{gx4}+\frac{1}{\Sigma^k_{Rg}}\left(\frac{\alpha^k_{gx}\cosh\left(\alpha^k_{gx}\right)}{m^k_{gx1}(\sinh)}-1\right)\right.$$

$$\left.\times\left(\frac{1}{\Delta y_k}\rho^k_{gyx1}+\frac{1}{\Delta z_k}\rho^k_{gzx1}-s^k_{gx1}\right)\right]+\frac{2D^{k+1}_g}{\Delta x_{k+1}}\left[3a^{k+1}_{gx2}+a^{k+1}_{gx4}\times\frac{\left(\alpha^{k+1}_{gx}\sinh\left(\alpha^{k+1}_{gx}\right)-3m^{k+1}_{gx2}(\cosh)\right)}{\left(\cosh\left(\alpha^{k+1}_{gx}\right)-m^{k+1}_{gxo}(\cosh)-m^{k+1}_{gx2}(\cosh)\right)}\right.$$

$$\left.-\frac{1}{\Sigma^{k+1}_{Rg}}\left(\frac{\alpha^{k+1}_{gx}\cosh\left(\alpha^{k+1}_{gx}\right)}{m^{k+1}_{gx1}(\sinh)}-1\right)\left(\frac{1}{\Delta y_{k+1}}\rho^{k+1}_{gyx1}+\frac{1}{\Delta z_{k+1}}\rho^{k+1}_{gzx1}-s^{k+1}_{gx1}\right)\right].$$

As a result instead of the initial system of $8G$ equations for the two-node problem $(k, k+1)$ we have to solve only G neutron balance equations with respect to the second moments of $k+1$ node and $2G$ neutron flux and neutron current continuity equations with respect to the first moments of the two-node problem. Then, the third and the fourth moments can be calculated using the expressions (1) and (2). It is worth to mention that the numerical algorithm of the analytical nodal equations solution is more efficient than that of the nodal expansion method, where we have to solve $2G$ and $4G$ equations for each two-node problem (Engrand *et al.*, 1992).

After calculating neutron flux expansion coefficients we can obtain the nodal surface-averaged neutron current $J^{k,NOD}_{gx+}$ at the internal interface of the two-node problem as

$$J_{gx+}^{k,NOD} = -\frac{2D_g^k}{\Delta x_k}\left[a_{gx1}^k + 3a_{gx2}^k + \left[\frac{\alpha_{gx}^k \cosh\left(\alpha_{gx}^k\right) - m_{gx1}^k(\sinh)}{\sinh\left(\alpha_{gx}^k\right) - m_{gx1}^k(\sinh)}\right]a_{gx3}^k + \left[\frac{\alpha_{gx}^k \sinh\left(\alpha_{gx}^k\right) - 3m_{gx2}^k(\cosh)}{\cosh\left(\alpha_{gx}^k\right) - m_{gxo}^k(\cosh) - m_{gx2}^k(\cosh)}\right]a_{gx4}^k\right].$$

Implementation of the nodal coupling into the CMFD equations has been performed by the same way as in the NESTLE code (Maldonado and Turinsky, 1995). The surface-average finite-difference neutron current $J_{gx+}^{k,FDM}$ is expressed as follows:

$$J_{gx+}^{k,FDM} = -\mathrm{d}_{gx+}^{k,FDM}\left[\overline{\Phi}_g^{k+1} - \overline{\Phi}_g^k\right] - \mathrm{d}_{gx+}^{k,NOD}\left[\overline{\Phi}_g^{k+1} + \overline{\Phi}_g^k\right],$$

where $\mathrm{d}_{gx+}^{k,FDM}$ denotes the finite-difference coupling coefficient, $\mathrm{d}_{gx+}^{k,NOD}$ is the nodal coupling coefficient. By setting $J_{g,x+}^{k,FDM} = J_{g,x+}^{k,NOD}$, the nodal coupling coefficients can be computed from

$$\mathrm{d}_{gx+}^{k,NOD} = -\frac{\left[\mathrm{d}_{gx+}^{k,FDM}\left(\overline{\Phi}_g^{k+1} - \overline{\Phi}_g^k\right) + J_{gx+}^{k,NOD}\right]}{\left(\overline{\Phi}_g^{k+1} + \overline{\Phi}_g^k\right)}.$$

The resulting CMFD neutron diffusion equations are as follows:

$$\sum_{u=x,y,z} S_u^k\Big[-\left(\mathrm{d}_{g,u-}^{k,FDM} - \mathrm{d}_{g,u-}^{k,NOD}\right)\overline{\Phi}_g^{j-} - \left(\mathrm{d}_{g,u+}^{k,FDM} + \mathrm{d}_{g,u+}^{k,NOD}\right)\overline{\Phi}_g^{j+} + \left(\mathrm{d}_{g,u-}^{k,FDM} + \mathrm{d}_{g,u-}^{k,NOD}\right)\overline{\Phi}_g^k$$

$$+\left(\mathrm{d}_{g,u+}^{k,FDM} - \mathrm{d}_{g,u+}^{k,NOD}\right)\overline{\Phi}_g^k\Big] + \Sigma_{Rg}^k\overline{\Phi}_g^k V_k = \chi_g\sum_{g'=1}^{G}\nu\Sigma_{fg'}^k\overline{\Phi}_{g'}^k V_k + \sum_{g'\neq g}^{G}\Sigma_{sg'\to g}^k\overline{\Phi}_{g'}^k V_k + \overline{S}_g^k V_k$$

where index $j\pm$ refers to the nodes adjacent to the node k in $u\pm$ direction.

3. REDUCTION OF THE NEUTRON KINETICS EQUATIONS TO THE FSP FORM

The transverse-integrated few-group neutron kinetics equations can be written in the x-direction as follows:

$$\frac{1}{v_g}\frac{\partial\Phi_g^k(x,t)}{\partial t} = D_g^k(t)\frac{\mathrm{d}^2}{\mathrm{d}x^2}\Phi_g^k(x,t) - \Sigma_{Rg}^k(t)\Phi_g^k(x,t) + (1-\beta)\chi_g^{(p)}\sum_{g'=1}^{G}\nu\Sigma_{fg'}^k(t)\Phi_{g'}^k(x,t)$$
$$+\sum_{g'\neq g}\Sigma_{sg'\to g}^k(t)\Phi_{g'}^k(x,t) - \frac{1}{\Delta y_k}L_{gy}^k(x,t) - \frac{1}{\Delta z_k}L_{gz}^k(x,t) \qquad (3)$$
$$+\sum_{j=1}^{J}\lambda_j\chi_{gj}^{(\mathrm{d})}C_j^k(x,t), \qquad g = 1,\ldots,G;$$

$$\frac{\partial C_j^k(x,t)}{\partial t} = \beta_j \sum_{g'=1}^{G} \nu\Sigma_{fg'}^k(t)\Phi_{g'}^k(x,t) - \lambda_j C_j^k(x,t), \qquad j = 1,\ldots,J; \qquad (4)$$

where the notation is fairly standard.

The system of equations (3) and (4) is completed by suitable boundary and initial conditions. To obtain a numerical solution of the initial problem, equations (3) and (4) have to be discretized in space and time. An analytical treatment of the delayed neutron precursors equations in combination with the fully implicit scheme for the neutron flux equations (Stacey, 1969) is used as a time discretization technique. The delayed neutron precursor equations are integrated over the time interval $[t, t+\Delta t]$ assuming a linear dependence of the neutron flux. The result follows as

$$C_j^k(x,t+\Delta t) = C_j^k(x,t)\exp(-\lambda_j\Delta t) + \frac{\beta_j}{\lambda_j}\left\{\sum_{g'=1}^{G}\nu\Sigma_{fg'}^k(t)\Phi_{g'}^k(x,t)\left[\frac{1-\exp(-\lambda_j\Delta t)}{\lambda_j\Delta t} - \exp(-\lambda_j\Delta t)\right]\right.$$
$$\left. + \sum_{g'=1}^{G}\nu\Sigma_{g'}^k(t+\Delta t)\Phi_{g'}^k(x,t+\Delta t)\left[1 - \frac{1-\exp(-\lambda_j\Delta t)}{\lambda_j\Delta t}\right]\right\}$$

Substituting this expression into the neutron flux equation (3) and using the fully implicit scheme for the neutron flux derivative we obtain the time-discretized neutron flux equations as

$$\frac{\Phi_g^k(x,t+\Delta t)}{v_g\Delta t} - D_g^k(t+\Delta t)\frac{d^2}{dx^2}\Phi_g^k(x,t+\Delta t) + \Sigma_{Rg}^k(t+\Delta t)\Phi_g^k(x,t+\Delta t)$$
$$- \sum_{g'\neq g}\Sigma_{sg'\to g}^k(t+\Delta t)\Phi_{g'}^k(x,t+\Delta t) - \chi_g^{\mathrm{NEW}}\sum_{g'=1}^{G}\nu\Sigma_{fg'}^k(t+\Delta t)\Phi_{g'}^k(x,t+\Delta t)$$
$$+ \frac{1}{\Delta y_k}L_{gy}^k(x,t+\Delta t) + \frac{1}{\Delta z_k}L_{gz}^k(x,t+\Delta t) = S_g^k(x,t) \qquad (5)$$

where

$$S_g^k(x,t) = \frac{1}{v_g\Delta t}\Phi_g^k(x,t) + \chi_g^{\mathrm{OLD}}\sum_{g'=1}^{G}\nu\Sigma_{fg'}^k\Phi_{g'}^k(x,t) + \sum_{j=1}^{J}\chi_{gi}^{(\mathrm{d})}\lambda_j C_j^k(x,t)\exp(-\lambda_j\Delta t)$$

$$\chi_g^{\mathrm{NEW}} = (1-\beta)\chi_g^{(p)} + \sum_{j=1}^{J}\beta_j\chi_{gj}^{(\mathrm{d})}\left(1 - \frac{1-\exp(-\lambda_j\Delta t)}{\lambda_j\Delta t}\right)$$

$$\chi_g^{\mathrm{OLD}} = \sum_{j=1}^{J}\beta_j\chi_{gj}^{(\mathrm{d})}\left(\frac{1-\exp(-\lambda_j\Delta t)}{\lambda_j\Delta t} - \exp(-\lambda_j\Delta t)\right).$$

As a result we have the FSP equations similar to the equations of the steady-state FSP considered in Section 2. If we want to use the analytical nodal method to the equation (5)

in a straightforward way we have to know the higher order coefficients of the neutron flux and delayed neutron precursors from the previous time-step. That would eliminate one of advantages of the nonlinear iteration procedure—the computer memory storage reduction. In order to save this advantage we follow the method proposed by Engrand *et al.* (1992) for the NESTLE code. In their approach the neutron kinetics FSP equations are led to the steady-state FSP equations grouping all additional terms into the source term. As a result we have

$$-D_g^k(t+\Delta t)\frac{\mathrm{d}^2}{\mathrm{d}x^2}\Phi_g^k(x,t+\Delta t)+\Sigma_{Rg}^k(t+\Delta t)\Phi_g^k(x,t+\Delta t)=\sum_{g'\neq g}\Sigma_{sg'\to g}^k(t+\Delta t)\Phi_{g'}^k(x,t+\Delta t)$$

$$+\chi_g^{(p)}\sum_{g'=1}^{G}\nu\Sigma_{fg'}^k(t+\Delta t)\Phi_{g'}^k(x,t+\Delta t)-\frac{1}{\Delta y_k}L_{gy}^k(x,t+\Delta t)-\frac{1}{\Delta z_k}L_{gz}^k(x,t+\Delta t)+S_g^k(x,t+\Delta t)$$

where

$$S_g^k(x,t+\Delta t)=\frac{1}{v_g\Delta t}\Phi_g^k(x,t)-\frac{1}{v_g\Delta t}\Phi_g^k(x,t+\Delta t)+\sum_{j=1}^{J}\chi_{gj}^{(\mathrm{d})}\lambda_j C_j^k(x,t)\exp(-\lambda_j\Delta t)$$

$$+\chi_g^{\mathrm{OLD}}\sum_{g'=1}^{G}\nu\Sigma_{fg'}^k(t)\Phi_{g'}^k(x,t)+\left(\chi_g^{\mathrm{NEW}}-\chi_g^{(p)}\right)\sum_{g'=1}^{G}\nu\Sigma_{fg'}^k(t+\Delta t)\Phi_{g'}^k(x,t+\Delta t).$$

The higher order coefficients of the source term expansion are calculated in the same way as the higher order coefficients of the transverse leakage terms using the quadratic leakage approximation.

4. AUTOMATIC TIME-STEP SIZE CONTROL

Most of the modern neutron kinetics codes use an automatic time-step size control procedure in order to obtain a solution with a given tolerance (Aviles, 1993; Taiwo *et al.*, 1993; Crouzet and Turinsky, 1996; Joo *et al.*, 1996). Moreover, a variable time-step size usually decreases a total amount of time-steps and respectively computing time. We use a standard time-step doubling strategy (Hairer *et al.*, 1987) in order to estimate a temporal truncation error and to predict a time-step size. The procedure is mathematically well-founded and described in details elsewhere (Hairer *et al.*, 1987; Joppich and Mijalkovic, 1993; Crouzet and Turinsky, 1996), we only briefly outline the main features.

Time integration from the time moment t_j is performed on the two temporal meshes: on the fine mesh with time-step size Δt_j and on the coarse one with time-step size $2\Delta t_j$. As a result at the time moment $t_j+2\Delta t_j$ we have two solutions: $\Phi_{\Delta t_j}$ and $\Phi_{2\Delta t_j}$, respectively. The local error of the fully implicit scheme can be expressed as follows:

$$\mathrm{Err}=C\Delta t^2+O(\Delta t^3) \tag{6}$$

where C is proportional to a second derivative of the neutron flux.

Applying the Richardson extrapolation for two obtained solutions and neglecting the higher order terms we can obtain the temporal truncation error of the solution $\Phi_{\Delta t_j}$ as

$$\mathrm{Err} = \left\| \Phi_{\Delta t_j} - \Phi_{2\Delta t_j} \right\|. \tag{7}$$

A most appropriate norm in the expression (7) is the L_∞-norm if we want to hold the temporal error within a given tolerance in the whole reactor domain. However an application of the L_2-norm demonstrates more robust qualities for the time-step size selection (Joppich and Mijalkovic, 1993; Crouzet and Turinsky, 1996) and we applied this norm for the error estimates. In addition, the error which has to be controlled is a relative one and the expression (7) is replace on the following one as

$$\mathrm{Err} = \left\| \Phi_{\Delta t_j} - \Phi_{2\Delta t_j} \right\| / \left\| \Phi_{\Delta t_j} \right\|.$$

Using the expression (6) and requiring that the temporal truncation error should be equal to the prescribed tolerance Tol we get a prediction of the new time-step size as

$$\Delta t^{\mathrm{NEW}} = \sqrt{\frac{\mathrm{Tol}}{\mathrm{Err}}} \Delta t_j.$$

A time-step acceptance criterion can be written in the form

$$\mathrm{Err} \leq \mathrm{Tol}.$$

If the estimated error satisfies the above criterion, the jth time-step is accepted and $\Delta t_{j+1} = \Delta t^{\mathrm{NEW}}$ is used as a next time-step size. Otherwise the current time-step is rejected and repeated with $\Delta t_j = \Delta t^{\mathrm{NEW}}$.

In order to avoid repeated time-step size rejections the safety parameters are introduced. The new time-step size is calculated from

$$\Delta t^{\mathrm{NEW}} = \Delta t_j \min\left(\mathrm{Facmax}, \max\left(\mathrm{Facmin}, \mathrm{Safety}\frac{\Delta t^{\mathrm{NEW}}}{\Delta t_j}\right)\right).$$

The Facmax and Facmin are usually equal to 2 and 0.5. The typical value of the parameter Safety is in the range 0.8–0.9.

5. ITERATIVE SOLUTION PROCEDURE

The neutron kinetics equations at each time-step are solved iteratively using three levels of embedded iterations: the nonlinear iterations, the outer and inner iterations as it is illustrated at Fig. 1. At the nonlinear iteration the two-node nodal equations are solved and the coarse-mesh nodal coupling coefficients are recomputed. The solution of the resulting CMFD equations is performed using traditional outer and inner iterations. The outer iterations are performed by the Chebyshev acceleration procedure (Zimin and Ninokata, 1996). The procedure allows us to realize two iterative methods: the classical Chebyshev

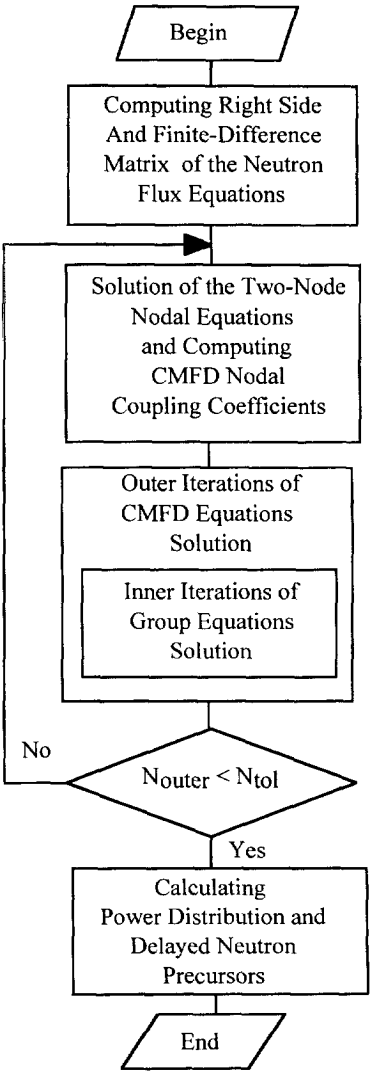

Fig. 1. Flow diagram of the neutron kinetics time-step.

semi-iterative (CSI) method (Hageman and Young, 1981) and the Chebyshev semi-analytical (CSA) method (Zimin and Ninokata, 1996). In the CSA method the Chebyshev polynomials are chosen to optimize the convergence of the residual vectors to the first eigenvector of the iteration matrix. When the convergence is attained, the 'exact' solution is obtained by adding an error vector to the iterative approximation. The relative efficiency of the CSA method in comparison with the CSI method is determined by the dominance ratio of the iteration matrix. A detail description of the Chebyshev outer acceleration procedure and the CSA method is given in our previous paper (Zimin and Ninokata, 1996). We would like only to note that the 'optimal' initial approximation

(Zimin and Ninokata, 1996) proposed for the CSA method demonstrated a breakdown during nonlinear iterative process. All performed calculations presented below are started with a zero initial approximation for the neutron flux at each time-step.

The following convergence criteria are applied. A number of inner iterations performed by SSOR method is fixed to two for the both neutron energy groups. The outer iterations are executed till the tolerance 10^{-4}. The global iterations are terminated if a number of outer iterations is less or equal to 8.

6. NUMERICAL RESULTS

The described numerical methods are implemented into the neutron kinetics computer code SKETCH-N. Verification of the code is performed against the LWR benchmark problems: the 3D Langenbuch–Maurer–Werner (LMW) problem (Langenbuch *et al.*, 1977) and 2D and 3D BWR Laboratorium fur Reaktorregelung und Anlagensicherung (LRA) super-prompt-critical transients (Argonne National Laboratory, 1977). The comparison of the SKETCH-N calculations is done with the other nodal computer code results available from the literature. All SKETCH-N computations have been carried out on the DEC 3000 AXP model 400 workstation.

6.1. 3D Langenbuch–Maurer–Werner operational transient

The LMW problem is an operational transient in an LWR model (Langenbuch *et al.*, 1977). The small-sized two-zone core consists of 77 assemblies, surrounded radially and axially by a water reflector. The transient is initiated by withdrawing a bank of four partially inserted control rods at the rate of 3 cm s^{-1} over the time interval from 0 to 26.7 s. The second bank of control rods is inserted at the same rate over the time from 7.5 to 47.5 s. The transient is followed for 60 s. The numerical solution of this problem had been obtained using several nodal computer codes (Langenbuch *et al.*, 1977, Sutton and Aviles, 1996). All nodal code results used for the comparison are taken from (Sutton and Aviles, 1996).

In order to separate spatial and temporal truncation errors of the SKETCH-N code we performed two sets of the calculations. The first calculations are done with different spatial mesh sizes and time-step size 0.25 s. The PANTHER code (Hutt and Knight, 1993) results with $11\times11\times40$ spatial mesh and 0.25 s time-step size are considered as a reference solution. The PANTHER solution and the SKETCH-N results with the meshes $6\times6\times10$, $6\times6\times20$, $11\times11\times40$ are presented in Table 1. The QUANDRY code (Smith, 1979) solution is also given for the comparison. We can see that the SKETCH-N calculations with 20 cm mesh size give 3.5% of the maximum error in the reactor-averaged power destiny. The reason, we believe, is mostly due to an approximate treatment of the nodes with a partially inserted control rod, which is called a rod cusping effect. The volume-weighting homogenization of the macroscopic cross-sections is used for these nodes and that can be a main reason of the errors. The assumption is confirmed by the calculation with 10 cm mesh size in axial direction (mesh $6\times6\times20$). The errors in this case are significantly smaller. The difference between the PANTHER and SKETCH-N results with the same mesh size lies below 1% and can be explained by the differences in the space and time discretization methods.

Table 1. Results of the 3D LMW LWR benchmark problem obtained with different spatial meshes. Time-step size is equal to 0.25 s for all calculations

Code	PANTHER	QUANDRY	SKETCH-N	SKETCH-N	SKETCH-N
Mesh	11×11×40	6×6×20	6×6×10	6×6×20	11×11×40
Eigenvalue	—	—	0.99956	0.99955	0.99950
No. of nonlinear iterations/time-step	—	—	3	3	2
No. of outer iterations/nonlinear	—	—	14	13	18
CPU time (s)	—	—	88	168	1126
Time (s)	Average power density (W cm^{-3}) (deviation from the PANTHER results (%))				
10.0	202.1	202.0 (−0.0)	197.6 (−2.2)	200.7 (−0.7)	201.0 (−0.5)
20.0	258.9	260.5 (1.3)	250.5 (−3.2)	255.8 (−1.2)	257.2 (−0.6)
30.0	207.3	209.9 (1.7)	200.0 (−3.5)	205.3 (−1.0)	206.7 (−0.3)
40.0	122.0	123.9 (0.8)	119.0 (−2.5)	121.3 (−0.6)	121.9 (−0.1)
50.0	75.7	76.5 (0.0)	74.0 (−2.2)	75.3 (−0.5)	75.6 (−0.1)
60.0	58.1	58.6 (−0.3)	56.8 (−2.2)	57.8 (−0.6)	58.0 (−0.2)

Table 1 also includes the average number of nonlinear iterations per time-step and the average number of outer iterations per nonlinear one. The decrease of the spatial mesh size influences the iterative processes in two opposite ways: on the one hand the second eigenvalue of the iteration matrix is increasing, which deteriorates the convergence of the CSA method used as an outer iteration technique; on the other hand the nonlinear nodal coupling coefficients are decreasing, which improves the convergence of the nonlinear iterations. These theoretical considerations are confirmed by the presented numerical results.

The second set of the SKETCH-N calculations has been performed in order to estimate the fully implicit scheme used in the code. The mesh structure is fixed to 6×6×20. The computations with constant time-step sizes 1, 2.5, 5 s and using automatic step size control procedure are done. In order to eliminate the spatial discretization errors the comparison of the obtained results is performed against the SKETCH-N calculation with the same spatial mesh size and 0.25 s time-step size (see Table 1). The results are presented in Table 2. The temporal truncation errors are very small even in the case of the large time-step size. The numerical results show that the number of nonlinear iterations per time-step and the number of outer iterations per nonlinear one are slightly increasing with the increase of the time-step size.

6.2. 2D BWR LRA Super-prompt-critical transient

The second problem is a super-prompt-critical transient in a simplified BWR model proposed by the LRA (Argonne National Laboratory, 1977). The quarter-core reactor model is illustrated in Fig. 2. The transient is initiated by a drop of the peripheral control rod at the low reactor power. The control rod movement is simulated by a linear decrease of the thermal group absorption cross-section at the four fuel assemblies adjacent to the control rod marked by letter R in Fig. 2. The control rod is fully withdrawn from the core

Table 2. SKETCH-N results of the 3D LMW LWR problem computed with the different time-step sizes. Spatial mesh is 6×6×20

Time-step size (s)	1	2.5	5	Variable (Tol = 10^{-2})	Variable (Tol = 10^{-1})
No. of time-steps	60	24	12	26(0)†	12(0)†
No. of nonlinear iterations/time-step	4	4	5	4	5
No. of outer iterations/nonlinear	14	15	15	14	15
CPU time (s)	54	25	15	40	23
Time (s)	Temporal truncation error of the average power density‡ (%)				
10.0	0.05	0.3	1.0	0.3	1.0
20.0	−0.01	0.0	−0.3	0.0	−0.3
30.0	−0.06	−0.3	−1.5	−0.2	−1.5
40.0	−0.01	−0.1	−0.6	0.0	−0.6
50.0	0.03	0.1	0.4	0.2	0.4
60.0	0.01	0.1	0.2	0.2	0.2

†Number in brackets denotes the number of time-steps discarded by the automatic time-step size control procedure.
‡Deviations from the SKETCH-N results with 0.25 s time-step size.

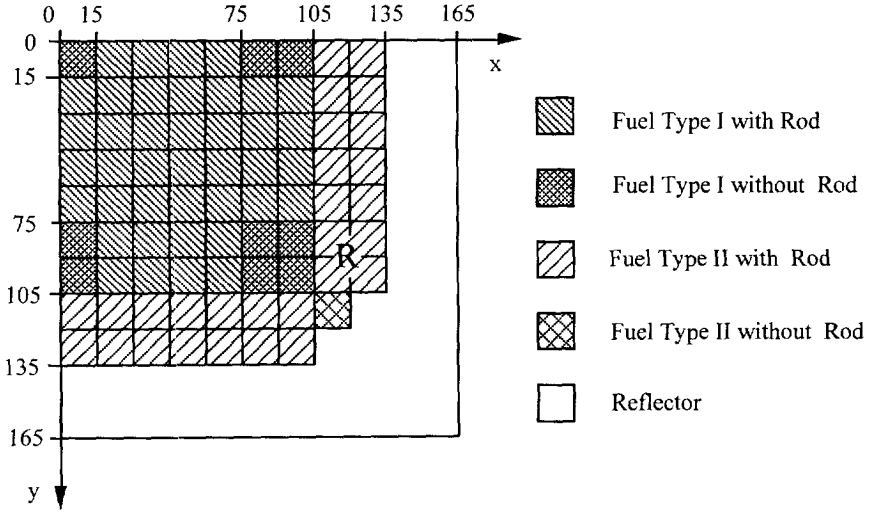

Fig. 2. Quadrant of the reactor core for 2D and 3D BWR LRA benchmark problems.

at the time 2.0 s. The transient is calculated for 3 s. The benchmark problem includes adiabatic heatup equations and a simple Doppler feedback model. A detailed description of the problem is given in Brega *et al.* (1981).

The problem has been calculated by the SKETCH-N code with 15 and 7.5 cm spatial mesh sizes and the temporal meshes generated by the automatic time-step size control

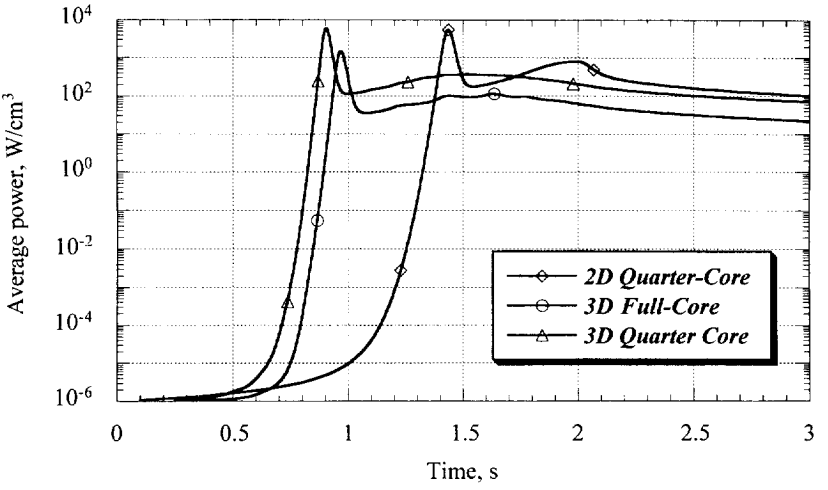

Fig. 3. Reactor-averaged power densities versus time for 2D and 3D BWR LRA problems.

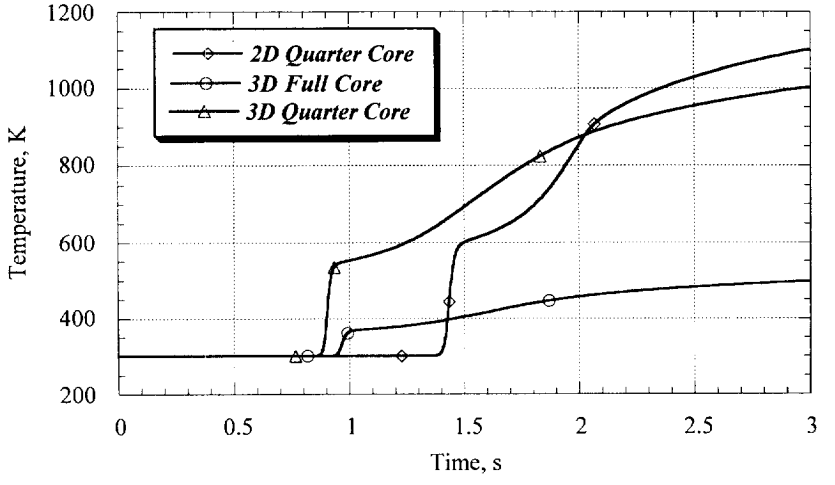

Fig. 4. Average fuel temperatures versus time for 2D and 3D BWR LRA problems.

procedure with the prescribed tolerances 10^{-2} and 10^{-3}. The reactor-averaged power density during the transient is shown at Fig. 3. Figure 4 demonstrates the reactor-averaged fuel temperature versus time. The most important transient parameters are summarized in Table 3. The QUANDRY (Smith, 1979), IQSBOX (Finnemann *et al.*, 1977) and TWOD-II (Shober *et al.*, 1977) results taken from (Song and Kim, 1995) are added for comparison. For all considered parameters there is very good agreement among the different codes. The coarse spatial mesh calculations give the slightly overestimated values of the first power peak and the fuel temperatures. The coarse temporal mesh calculations in comparison with the fine ones decrease the time of the first power peak and its value.

Table 3. Results of the 2D BWR LRA problem

Code	SKETCH-N	SKETCH-N	SKETCH-N	SKETCH-N	IQSBOX	QUANDRY	TWOD-II
Mesh	11×11	11×11	22×22	22×22	11×11	11×11	22×22
Eigenvalue	0.99635	0.99635	0.99638	0.99638	0.99631	0.99641	0.99636
No. of time-steps	634(3)†‡	2142(0)†§	630(3)†‡	2098(0)†§	522	1000	2600
Time of the first power peak (s)	1.437	1.443	1.434	1.439	1.455	1.435	1.438
Average power at the first peak (W cm^{-3})	5567	5616	5439	5481	5451	5473	5411
Average power at the 2nd peak (W cm^{-3})	818	820	800	801	~800	797	784
Average power at time 3 s (W cm^{-3})	103	102	100	99	~100	97.5	96.2
Average fuel temperature at time 3 s (K)	1119	1117	1102	1099	1127	1108	1087
Maximum fuel temperature at time 3 s (K)	3059	3057	2992	2986	2989	3029	2948
No. of nonlinear iterations/time-step	3.1	2.6	2.6	2.1	—	—	—
No. of outer iterations/nonlinear	17.8	15.8	18.7	17.6	—	—	—
Computer	DEC 3000	DEC 3000	DEC 3000	DEC 3000	CYBER 175	IBM 370/168	IBM 370/195
CPU time (s)	119	319	440	988	255	307	1661

† Values in ( ) denotes the number of discarded time-steps.
‡ Prescribed tolerance of the automatic time-step size control is equal to 10^{-2}.
§ Prescribed tolerance is equal to 10^{-3}.

The presented number of iterations confirms the conclusion of Section 6.1 that an increase in the time-step size increases insignificantly a number of nonlinear iterations per time-step and a number of the outer iterations per nonlinear one. A decrease in the spatial mesh size results in a decrease in the number of the nonlinear iterations and in an increase in the number of outer iterations.

6.3. 3D BWR LRA Super-prompt-critical transient. Quarter-core formulation

The problem is an extension of the 2D BWR LRA super-prompt-critical problem to three dimensions (Argonne National Laboratory, 1977). The active reactor core height is 300 cm. The core is surrounded by 30 cm of the axial reflector. All other data and models are the same as in the 2-dimensional case and are given in Brega *et al.* (1981). The quarter-core configuration has been considered. Two axially different spatial meshes are used. The spatial mesh size in x-direction is as follows: $\Delta x = 15$ cm for $0 \leq \times \leq 120$ cm, $\Delta x = 7.5$ cm for $120 \leq \times \leq 135$ cm, $\Delta x = 15$cm for $135 \leq \times \leq 165$ cm; the mesh size is the same in y-direction. The first axially coarse mesh is $12\times12\times14$ and has 14 axial layers with heights of 30, 15, 22.5 (2 layers), 30 (6 layers), 22.5 (2 layers), 15, 30 cm. The second axially fine mesh $12\times12\times28$ has 28 layers with heights of 20, 10, 7.5 (2 layers), 11.25 (4 layers), 15 (12 layers), 11.25 (4 layers), 7.5 (2 layers), 10, 20 cm. Three calculations of the problem have been performed: (1) with the $12\times12\times14$ spatial mesh and the temporal tolerance criterion 10^{-2}; (2) with the $12\times12\times28$ spatial mesh and the tolerance criterion 10^{-2}; (3) with the $12\times12\times28$ spatial mesh and the tolerance criterion 10^{-3}.

The reactor-averaged power density during the transient is shown at Fig. 3. Figure 4 demonstrates the reactor-averaged fuel temperature versus time. The most important parameters of the computations are given in Table 4. The QUANDRY solution taken from Brega *et al.* (1981) is also presented for a comparison. The results show that a rod cusping effect for the BWR LRA transient is less then for the LMW problem but also takes place. The coarse axial mesh size calculation has yielded a lower peak power value and delayed the time of its occurrence. The temporal truncation errors of the calculations with 10^{-2} tolerance criterion are found to be rather small. The SKETCH-N results and the QUANDRY results are in good agreement for all parameters except for the second peak power density values.

6.4. 3D BWR LRA super-prompt-critical transient. Full-core formulation

There is a variant of the 3D BWR LRA problem (Argonne National Laboratory, 1977), where the full core configuration is considered and the transient is initiated by an ejection only one control rod instead of four as is defined for the original problem. The SKETCH-N calculations have been carried out with two axially different meshes defined in Section 6.3. The reactor-averaged power density during the transient is shown at Fig. 3. Figure 4 demonstrates the reactor-averaged fuel temperature. The SKETCH-N results are given in Table 5, where the QUANDRY, PANTHER and SPANDEX results taken from Sutton and Aviles (1996) are also presented for comparison. The SKETCH-N solutions obtained with the axially coarse mesh and the axially fine mesh are practically identical, which shows that a rod cusping effect is rather small for the problem. There is also a very good agreement among all nodal code results.

Table 4. Results of the 3D BWR LRA problem. Quarter-core calculations

Code	SKETCH-N	SKETCH-N	SKETCH-N	QUANDRY
Mesh	12×12×14	12×12×28	12×12×28	12×12×14
Eigenvalue	0.99637	0.99638	0.99638	0.99644
No. of time-steps	726(6)†‡	718(5)†‡	2670(9)†§	2708
Time to the first power peak (s)	0.9188	0.9044	0.9085	0.9140
Power density at the fist peak (W cm ^{3})	5367	5914	5946	5332
Time to the first minimum (s)	1.027	0.994	0.996	1.00
Power density at the first minimum (W cm^{-3})	129.8	110.8	113.4	128.2
Time of the second power peak (s)	1.625	1.519	1.516	1.446
Power density at the 2nd peak (W cm^{-3})	379	366	365	432.9
Power density at time 3 s (W cm ^{3})	71.0	70.0	70.5	72.2
Average fuel temperature at time 3 s (K)	10021003	1003	1018	
Maximum fuel temperature at time 3 s (K)	4038	4070	4080	4120
No. of nonlinear iterations/time-step	3.5	2.9	2.5	—
No. of outer iterations/nonlinear	23.8	24.9	18.8	—
Computer	DEC 3000	DEC 3000	DEC 3000	IBM 370/158
CPU time (min)	64	104	294	720

† Values in ( ) denotes the number of discarded time-steps.
‡ Prescribed tolerance of the automatic time-step size control is equal to 10^{-2}.
§ Prescribed tolerance is equal to 10^{-3}.

Table 5. Results of the 3D BWR LRA problem. Full-core formulation

Code	SKETCH-N	SKETCH-N	QUANDRY	PANTHER	SPANDEX
Mesh	24×24×14	24×24×28	13×13×10	13×13×10	22×22×14
Eigenvalue	0.99637	0.99638	0.99657	—	0.99642
No. of time-steps	698(6)†‡	702(5)†‡	820	820	1430(66)†
Time to the first power peak (s)	0.967	0.949	0.950	0.950	0.956
Power density at the first peak (W cm^{-3})	1485	1486	1435	1514	1478
Time to the first power minimum (s)	1.09	1.05	1.08	1.08	1.06
Power density at the first minimum (W cm^{-3})	35.3	34.8	20.7	36.7	36.4
Time of the second power peak (s)	1.63	1.61	1.57	1.52	1.62
Power density at the 2nd peak (W cm^{-3})	112	103	141	170	109
Power density at time 3 s (W cm^{-3})	22.1	21.8	22.6	23.3	22.3
Average fuel temperature at time 3 s (K)	497	497	—	—	—
Maximum fuel temperature at time 3 s (K)	3841	3847	—	—	—
No. of nonlinear iterations/time-step	3.4	2.9	—	—	—
No. of outer iterations/nonlinear	25.8	26.5	—	—	—
Computer	DEC 3000	DEC 3000	—	—	—
CPU time (min)	259	539	—	—	—

† Values in ( ) denotes a number of discarded time-steps.
‡ Prescribed tolerance of the automatic time-step size control is equal to 10^{-2}.

7. CONCLUSIONS

The analytical nodal method is extended for the solutions of the steady-state fixed source problem (FSP) and the neutron kinetics equations. The nodal method is implemented into the computer code SKETCH-N developed for the LWR neutronics transient calculations. The nonlinear iteration procedure used in the code decouples the solution procedure into the solution of the nodal equations for two-node problems and global iterations of the CMFD method. An orthogonality of the analytical basic functions leads to an efficient algorithm of solution of the two-node problem nodal equations. If G is a number of neutron energy groups, the initial system of $8G$ nodal equations for the two-node problem is reduced to the G and $2G$ equations. A fully implicit scheme in combination with an analytical treatment of the delayed neutron precursors equations is applied as a time integration method. The time-discretized neutron kinetics equations are carried into the steady-state FSP form. As a result there is no need for saving the higher order neutron flux expansion coefficients and the computer memory requirement is reduced. An automatic time-step size control based on the time-step doubling technique is incorporated into the SKETCH-N code. An iterative solution procedure of the neutron kinetics equations at each time-step contains three levels of embedded iterations: the nonlinear iterations, the outer and inner iterations. At each nonlinear iterations the nodal equations for two-node problems are solved and the coupling coefficients of the CMFD matrix are recalculated. The solution procedure of the CMFD equations consists of the outer iterations performed by the Chebyshev acceleration procedure and the inner iterations of the SSOR method. The Chebyshev outer acceleration procedure allows to realize the Chebyshev semi-iterative method and the Chebyshev Semi-Analytical (CSA) method. In the CSA method the convergence of the residual vectors to the eigenvector of the iteration matrix is accelerated. When the convergence is attained the error vector is added to the iterative approximation to refine the solution.

The 3D LMW LWR operational transient and 2D and 3D BWR LRA super-prompt-critical benchmark problems have been calculated in order to verify the applied numerical method and to validate the SKETCH-N code. The comparison of the numerical results with the solutions obtained by the other nodal computer codes demonstrates good accuracy and efficiency of the SKETCH-N code. An automatic time-step size selection provides a fast and accurate solution of the widely varying LWR transients. The fully implicit scheme used in the code allows very large time-step sizes for delayed critical transients without a loss of precision. A few nonlinear iterations per time-step are required for the convergence, which confirms an efficiency of the nonlinear iteration procedure. The CSA method is specially efficient for the delayed critical transients with a large time-step size, when traditional iterative methods usually show slow convergence. The number of iterations does not significantly change when the spatial mesh size is decreasing and the time-step size is increasing.

The volume–weighting homogenization was used for the treatment of the partially rodded nodes during the transients. This approach results in some errors, known as a rod cusping effect. An application of the more consistent homogenization methods (Rajic and Ougouag, 1987; Takeda *et al.*, 1994) into the SKETCH-N code is under consideration.

Acknowledgements—Part of this work was done by the first author during his doctoral course study at Tokyo Institute of Technology sponsored by the Ministry of Education, Science, Sports

and Culture of Japan. The authors also wish to thank Professor T. Takeda of Osaka University, and Mr H. Ikeda and Mr A. Hotta, both of Toden Software Inc., for many stimulating discussions.

REFERENCES

Al-Chalabi, R. M., Turinsky, P. J., Faure, F. X., Sarsour, H. N. and Engrand, P. R. (1993) NESTLE: A Nodal Kinetics Code. *Transactions of American Nuclear Society* **68**, 432.

Al-Chalabi, R. M. and Turinsky, P. J. (1994) Application of Multigrid Method to Solving the NEM Form of Multigroup Neutron Diffusion Equation. *Transactions of American Nuclear Society* **71**, 259.

Argonne National Laboratory (1977) *Argonne Code Center Benchmark Problem Book.* Report ANL-7416, Suppl. 2.

Aviles, B. N. (1993) Development of a Variable Time-Step Transient NEM Code: SPANDEX. *Transactions of American Nuclear Society* **68**, 425.

Aviles, B. N. (1994) Importance of Variable Time-Step Algorithms in Spatial Kinetics Calculations. *Transactions of American Nuclear Society* **71**, 451.

Bennewitz, F., Finnemann, H. and Wagner, M. R. (1975) Higher Order Corrections in Nodal Reactor Calculations. *Transactions of American Nuclear Society* **22**, 173.

Borkowski, J., Smith, K., Hagrman, D., Kropaczek, D., Phodes III, J. and Esser, P. (1996) SIMULATE-3K Simulations of the Ringhals 1 BWR Stability Measurements. *Proceedings of the International Conference on the Physics of Reactors, PHYSOR 96*, 16–20 September, Mito, Ibaraki, Japan, p. J-121.

Brega, E., Di Pasquantonio, F. and Salina, E. (1981) Computation Accuracy and Efficiency of a Coarse-Mesh Analytic Nodal Method for LWR Transient Problems in Comparison with a Space–Time Synthesis Method. *Annals of Nuclear Energy* **8**, 509.

Crouzet, N. and Turinsky, P. (1996) A Second-Derivative-Based Adaptive Time–Step Method for Spatial Kinetics Calculations. *Nuclear Science and Engineering* **123**, 206.

Engrand, P. R., Maldonado, G. I., Al-Chalabi, R. M. and Turinsky, P. J. (1992) Nonlinear Iterative Strategy for NEM Refinement and Extension. *Transactions of American Nuclear Society* **65**, 221.

Finnemann, H., Bennewitz, F. and Wagner, M. R. (1977) Interface Current Techniques for Multidimensional Reactor Calculations. *Atomkernenergie*, **30**, 123.

Hageman, L. A. and Young, D. M. (1981) *Applied Iterative Methods.* Academic Press, New York.

Hairer, E., Norset, S. P. and Wanner, G. (1987) *Solving Ordinary Differential Equations I. Nonstiff Problems.* Springer-Verlag, Berlin.

Hennart, J. P. (1988) On Numerical Analysis of Analytical Nodal Methods. *Numerical Methods for Partial Differential Equations* **4**, 233.

Hutt, P. K. and Knight, M. P. (1993) The Improvement to the Transient Solution in the PANTHER Space–Time Code. *Transactions of American Nuclear Society* **68**, 427.

Ishii, Y. and Sano, H. (1996) Kinetic Analysis Program Based on a Nodal Expansion Method for Critical and Subcritical Reactors. *Proceedings of the International Conference on the Physics of Reactors, PHYSOR 96*, 16–20 September, Mito, Ibaraki, Japan, p. J-90.

Joo, H. G. and Downar, T. J. (1996) An Incomplete Domain Decomposition Preconditioning Method for Nonlinear Nodal Kinetics calculations. *Nuclear Science and Engineering* **123**, 403.

Joo, H. G., Downar, T. J. and Barber, D. A. (1996) Methods and Performance of a Parallel Reactor Kinetics Code PARCS. *Proceedings of the International Conference on the Physics of Reactors, PHYSOR 96*, 16–20 September, Mito, Ibaraki, Japan, p. J-42.

Joppich, W. and Mijalkovic, S. (1993) *Multigrid Methods for Process Simulation.* Springer-Verlag, New York.

Langenbuch S., Maurer, W. and Werner, W. (1977) Coarse-Mesh Flux-Expansion Method for the Analysis of Space–Time Effects in Large Light Water Reactor Cores. *Nuclear Science and Engineering* **63**, 437.

Lawrence, R. D. and Dorning, J. J. (1980) A Nodal Green's Function Method for Multidimensional Neutron Diffusion Calculations. *Nuclear Science and Engineering* **76**, 218.

Lawrence, R. D. (1986) Progress in Nodal Methods for the Solution of the Neutron Diffusion and Transport Equations. *Progress in Nuclear Energy*, **17**, 271.

Maldonado, G. I. and Turinsky, P. J. (1995) Application of Nonlinear Nodal Diffusion Generalized Perturbation Theory to Nuclear Fuel Reload Optimization. *Nuclear Technology* **110**, 198.

Rajic, H. L. and Ougouag, A. M. (1987) An Advanced Nodal Neutron Diffusion Method with Space-Dependent Cross Sections: ILLICO-VX. *Transactions of American Nuclear Society* **55**, 342.

Shober, R. A., Sims, R. N. and Henry, A. F. (1977) Two Nodal Methods for Solving Time-Dependent Group Diffusion Equations. *Nuclear Science and Engineering* **64**, 528.

Smith, K. S. (1979) *An Analytical Nodal Method for Solving the Two-Group, Multidimensional, Static and Transient Neutron Diffusion Equations.* Thesis, Nuclear Engineering MIT.

Smith, K. S. (1984) Nodal Method Storage Reduction by Nonlinear Iteration. *Transactions of American Nuclear Society* **44**, 265.

Song, J. W. and Kim, J. K. (1995) An Efficient Nodal Method for the Transient Calculations in Light Water Reactors. *Nuclear Technology* **110**, 198.

Stacey, W. M. (1969) *Space-Time Nuclear Reactor Kinetics.* Academic Press, New York.

Sutton, T. M. and Aviles, B. N. (1996) Diffusion Theory Methods for Spatial Kinetics Calculations. *Progress in Nuclear Energy* **30**, 119.

Taiwo, T. A., Khalil, H. S., Cahalan, J. E. and Morris, E. E. (1993) Time–Step Selection Considerations in the Analysis of Reactor Transients with DIF3D-K. *Transactions of American Nuclear Society* **68**, 429.

Takeda, T., Endo, T. and Takaya, H. (1994) Three-Dimensional Transient Analysis of Fast Reactors with Improved Coarse-Mesh Method. *Journal of Nuclear Science and Technology* **31**, 12.

Zimin, V. G. and Ninokata, H. (1996) Acceleration of the Outer Iterations of the Space-Dependent Neutron Kinetics Equations Solution. *Annals of Nuclear Energy* **23**, 1407.

Zimin, V. G. and Ninokata, H. (1997) Nonlinear Iteration Procedure Based on Legendre Polynomials. *Transactions of American Nuclear Society* **76**, 162.

Zimin, V. G. (1997) *Nodal Neutron Kinetics Models Based on Nonlinear Iteration Procedure for LWR Analysis.* Dr. Thesis, Nuclear Engineering, Tokyo Institute of Technology.

Yang, D. Y., Chen, G. S. and Chou, H. P. (1993) Application of Preconditioned Conjugate Gradient-Like Methods to Reactor Kinetics. *Annals of Nuclear Energy.* **20**, 9.